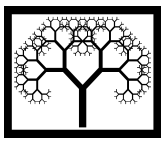

Proceedings of the Seventh International Conference
on Computational Structures Technology,
B.H.V. Topping and C.A. Mota Soares (Editors),
Civil-Comp Press, Stirling, Scotland.

Paper 164

A Comparison of Service Life Prediction of Concrete Structures using the Element-Free Galerkin, Finite Element and Finite Difference Methods

H. Taghaddos, F. Mahmoodzadeh, A. Noorzad, S. Mohammadi and A. Ansari
Department of Civil Engineering
University of Tehran, Iran

Abstract

Reinforced concrete structures exposed to sea environment conditions suffer from corrosion of steel bars due to chloride ingress. It is generally assumed that the diffusion of chloride ions follows the Fick's second low. Traditionally, such partial differential equations are solved using numerical methods, such as Finite Element Method (FEM) and Finite Difference Method (FDM). Although these methods are robust and efficient, they exhibit some numerical errors. In the present research, to decrease the numerical errors, Lagrange multiplier element-free Galerkin (EFG) method is applied to the partial differential equation of the Chloride diffusion. In this method, Moving Least Square (MLS) approximation is used to interpolate the field variable for a weak formulation of the boundary value problem. This approximation results continuity to the independent field variable, chloride content, and its gradient in the entire domain. In the present research, first the optimum scaling parameter of the support domain (d_{max}) and the weigh function's dilation parameter ($K_{ch)}$ in EFG method, which minimize the displacement error (L_2) and energy error (H_1) in 1D problem, are found and then the results, errors and predicted service life, are compared with the FE, the FD and available analytical solutions in special and practical situations.

Keywords: concrete, diffusion, service life, Fick's second low, mesh free, MLS, EFG, FEM, FDM.

1 Introduction

A lot of large infrastructures such as bridge and offshore structures are often exposed to several sea environments. Reinforced concrete structures exposed to sea environments suffer from corrosion of steel bars due to chloride ingress. The chloride penetration is a major factor that affects the durability of concrete structures. The durable life (or service life) of these structures have been determined

conventionally based on the initiation time to corrosion of steel bars, which is caused by penetrated amount of chlorides [1, 2].
Chloride diffusion analysis is required to determine the amount of chloride penetration at the location of steel bars. If the amount of penetrated chloride at the steel reinforcement reaches the limiting threshold value for corrosion, then the reinforcing bars start to corrode. The initiation period is the time that it takes for sufficient chlorides to penetrate the concrete cover to initiate corrosion. In other words, it represents the time taken chloride content at the cover's depth to reach the critical threshold concentration [3].
The accurate determination of chloride profile and a good estimation of the initiation period in concrete structures require an appropriate chloride diffusion analysis. So a newly developed method called element free Galerkin method is used for the first time to analyze the partial differential equation of the Chloride diffusion.

2 Chloride diffusion model

The diffusion of chloride ions is generally assumed to follow the Fick's second Low. The general diffusion equation can be written as follows [2]:

$$\frac{\partial C}{\partial t} = D(t)\nabla^2 C \tag{1}$$

Where;
C = chloride content in concrete
D = chloride diffusion coefficient
x = depth (from the exposed surface)
t = exposure time
The chloride diffusion coefficient is a function of both time and temperature:

$$D(t,T) = D_{ref}\left(\frac{t_{ref}}{t}\right)^m \exp\left[\frac{U}{R}\left(\frac{1}{T_{ref}} - \frac{1}{T}\right)\right] \tag{2}$$

Where;
$D(t,T)$ = diffusion coefficient at time t and temperature T
D_{ref} = diffusion coefficient at some reference time (t_{ref}) and temp (T_{ref})
m = a constant depending on mix proportions such as water-cementations material ratio and the type and proportion of cementations materials
U = activation energy of the diffusion process (35000 J/mol)
R = gas constant
T = absolute temperature
In the basic mode t_{ref} = 28 days and T_{ref} = 293°K (20°C). The temperature T of the concrete varies with time according to the geographic location.
The chloride exposure conditions (e.g. rate of chloride build up at the surface and maximum chloride content) are selected based on the type of structure (e.g. bridge deck, parking structure), the type of exposure (e.g. to marine or deicing salts) and

the geographic location. Maximum surface chloride concentration, C_s, and the time taken to reach that maximum, build up rate, is based on the type of structure and its geographic location. Since the diffusion is the main mechanism in the submerged zone we assume that build up rate equals to zero.

3 Solving the diffusion equation

In the present study, FDM, FEM and EFG methods are developed, implemented and compared to solve the diffusion equation in 1D cases. For the special cases of constant diffusion coefficient, the results are compared with the analytical solution.

3.1 Solving the diffusion equation with FEM

Algorithm of solving advection (convection) diffusion equation could be found in the literature [3, 4]. Here diffusion equation without the additional term of advection is discretized using a Galerkin weak form method for 1D problems.
Diffusion equation in Cartesian coordinate system can be written as:

$$L(C) = \frac{dC}{dt} - D\frac{\partial^2 C}{\partial x^2} \tag{3}$$

And by choosing ϕ_i as the shape function, the equivalent weak form is:

$$\int_{\Omega} \phi_i L(C) d\tau = \int_{\Omega} \phi_i \left[\frac{dC}{dt} - D\frac{\partial^2 C}{\partial x^2} \right] d\tau = \int_{\Omega} \phi_i \left[\frac{dC}{dt} + \frac{d\phi_i}{\partial x} D\frac{\partial C}{\partial x} \right] d\tau - D\int_{\partial\Omega} \phi_i \frac{\partial C}{\partial x} d\sigma = 0 \tag{4}$$

In addition, by dividing the entire domain Ω into elements Ω_e we will have:

$$S_e \left(\int_{\Omega_e} [\Phi][\Phi]^T d\tau \{Q'\}_e + \int_{\Omega_e} \frac{d[\Phi]}{dx} D\frac{d[\Phi]^T}{dx} d\tau \{Q\}_e - \int_{\partial\Omega_e} [\Phi] D\frac{\partial C}{\partial x} d\sigma \right) = 0 \tag{5}$$

The final system of linear algebraic equation can be derived as:

$$[M]\{Q\}' + [K]\{Q\} = \{b\} \tag{6}$$

Where:

$$[M] = \int_{\Omega_e} [\Phi][\Phi]^T d\tau \; ; \; [K] = \int_{\Omega_e} \frac{\partial[\Phi]}{\partial x} D\frac{\partial[\Phi]^T}{\partial x} d\tau \; ; \; [b] = \int_{\partial\Omega_e} [\Phi] D\frac{\partial C}{\partial x} d\sigma \tag{7}$$

Then the time interval [0, t] is subdivided into a finite number of equal subintervals Δt. By using Wilson-Teta equation we have:

$$([M]+\theta\Delta t[K])\{\Delta Q\}^{n+1} = -\Delta t[K]\{Q\}^{n} + \Delta t(\theta\{b\}^{n+1} + (1-\theta)\{b\}^{n}) \quad (8)$$

Equation 6 can be converted to equation 9 by defining new effective matrices:

$$K_{eff}\{\Delta Q\}^{n+1} = P_{eff} \quad (9)$$

Where:

$$K_{eff} = [M]+\theta\Delta t[K] \quad (10)$$

$$P_{eff} = -\Delta t[K]\{Q\}^{n} + \Delta t(\theta\{b\}^{n+1} + (1-\theta)\{b\}^{n}) \quad (11)$$

Equation (9) has to be solved in each time step to derive the chloride content, Q, at the end of the interval.
Finally by choosing linear shape function for the finite elements:

$$[\Phi] = \frac{1}{2}\begin{bmatrix} 1-\zeta \\ 1+\zeta \end{bmatrix} \quad (12)$$

K and M matrices can be derived:

$$[M] = \frac{L}{6}\begin{bmatrix} 2 & 1 \\ 1 & 2 \end{bmatrix} \quad , \quad [K] = \frac{D}{L}\begin{bmatrix} 1 & -1 \\ -1 & 1 \end{bmatrix} \quad (13)$$

Where L is the length of each element and D is the diffusion coefficient in each time step.
And b is a null vector due to symmetry.

3.2 Solving the diffusion equation with EFGM

The Galerkin weak form formulation, explained in the previous section can be easily used for mesh free solutions. The only major difference is the way the shape functions are formed. In FEM, the shape functions and discretized vectors belong to a specify element but in EFGM no specific element is defined and the vectors are evaluated over a specified domain.

3.2.1 EFG shape function (Moving least square)

EFG employs moving least-square (MLS) approximation to generate the shape functions. The central idea of MLS is that a global approximation can be achieved by going through a “moving” process. These approximations are constructed from three components: a weight function associated to each node, a basis, usually a polynomial one, and a set of coefficient that depends on the position [5].

The weight function is nonzero only over a small sub domain around the node I, so it defines a domain of influence Ω_i where it contributes to the approximation. The weight function of Gaussian type with a circular support is adopted for the MLS approximation because its partial derivatives exist to any desired order [6,7]. It takes the form of:

$$w_i(x,y) = \begin{cases} \dfrac{\exp(-(d_i/c)^2) - \exp(-(r/c)^2)}{1-\exp(-(r/c)^2)} & d_i \le r \\ 0 & d_i \ge r \end{cases} \tag{14}$$

Where $d_i = |x - x_i|$ is the distance of node x_i to a sampling point x in the support domain with radius r, and c= r/k_{ch} is the dilation parameter. The size of domain of influence at a node, d_{mI} is computed by

$$d_{mI} = d_{max}\, c_I \tag{15}$$

Where d_{max} is a scaling parameter and c_I is nodal spacing in a regular domain.

3.2.2 Applying Galerkin method

Applying the Galerkin method to the diffusion equation,

$$K_{ij} = \int_\Omega \nabla\Phi_i \nabla\Phi_j d\Omega \; M_{ij} = \int_\Omega \Phi_i \Phi_j d\Omega \quad , \quad K_{eff} = [M] + \theta\Delta t D[K] \tag{16}$$

$$P_{eff} = -\Delta t D[K]\{Q\}^n + \Delta t(\theta\{b\}^{n+1} + (1-\theta)\{b\}^n) \tag{17}$$

Which are similar to equations (7-11) with the difference that FEM shape functions are replaced by EFG shape functions.
It should be noted that the MLS shape functions do not satisfy the Kronecker delta criterion: $\Phi_i(x_j) \neq \delta_{ij}$, so the nodal parameters are not the nodal values. This complicates the imposition of boundary conditions if compared to the FEM. In this work the Lagrange Multiplier technique is used to impose the essential boundary conditions:

$$\delta\Delta Q^Y [K_{eff}\Delta Q + G\lambda - P_{eff}] + \delta\lambda^T (G^T \Delta Q - q] = 0 \tag{18}$$

Resulting in:

$$\begin{bmatrix} K_{eff} & G \\ G^T & 0 \end{bmatrix} \begin{bmatrix} \Delta Q \\ \lambda \end{bmatrix} = \begin{bmatrix} P_{eff} \\ q \end{bmatrix} \tag{19}$$

Where K_{eff} and P_{eff} are defined by (16-17) and G and q are evaluated at the boundary node k:

$$G_{IK} = -\Phi_k \Big|_{\Gamma_{uI}} \tag{20}$$

$$q_K = -\overline{\Delta Q}_k \tag{21}$$

Where $\overline{\Delta Q}$ is the specified value on the Dirichlet boundary (Γ_u), Φ_i is the MLS shape function of the i^{th} node, λ is the Lagrange Multiplier.
A regular structure system of cells is used for numerical integration using standard Gaussian quadrature is used at each cell.
The domain of influence of function associated to each node is defined by its weight function. Its size is defined by $R_I = \alpha d_I$ where α is a scaling parameter and $d_I = \max_{j \in S_j} \|x_J - x_I\|$, where S_J is a minimum set of neighboring points of x_I [10].
Therefore, for each integration point, a list of nodes, whose support includes the integration point, is required. Then, all the nonzero contributions in the Galerkin equations are evaluated. The result is a local matrix for the integration point, which should be assembled into the global matrix. The solution of the problem is obtained through the solution of the global system of equations [6].
It should be noted that the critical time step to have a stable result in FEM and EFG is given in the literatures [7].

3.3 Solving the diffusion equation with FDM

The most common method to solve diffusion equation is FDM. This method is explained completely in the literatures [7] and here we briefly point to this method. In this method, the region X-T, in 1D problem, is covered by a grid of rectangles of sides δX, δT. We assume that the coordinate of a representative grid point (X, T) is (iδX, jδT) and the value of C at this point is denoted by $C_{i,j}$. In the explicit method, by using Taylor's series in the T direction but keeping X constant, we have:

$$C_{i,j+1} = C_{i,j} + \delta T (\frac{\partial C}{\partial T})_{i,j} + \frac{1}{2} \delta T^2 (\frac{\partial^2 C}{\partial T^2})_{i,j} + ... \tag{22}$$

From which it follows that

$$(\frac{\partial C}{\partial T})_{i,j} = \frac{C_{i,j+1} - C_{i,j}}{\delta T} + O(\delta T) \tag{23}$$

Similarly by applying Taylor's series in the X direction, keeping T constant, we have:

$$(\frac{\partial^2 C}{\partial X^2})_{i,j} = \frac{C_{i+1,j} - 2C_{i,j} + C_{i-1,j}}{(\delta X)^2} + O(\delta X)^2 \quad (24)$$

By substituting (23) and (24) in (22) and neglecting the error terms, we have:

$$C_{i,j+1} = C_{i,j} + D\frac{\delta T}{(\delta X)^2}(C_{i-1,j} - 2C_{i,j} + C_{i+1,j}) \quad (25)$$

Which the stability restriction is $D\frac{\delta T}{(\delta X)^2} \le \frac{1}{2}$

3.4 Analytical Solution in the special situation

Assuming that diffusion coefficient is constant (m=0), analytical solution of the equation (1) in 1D cases with the following initial and boundary condition:

$$\begin{aligned} &I.C: \ C = 0, \qquad 0 < x < l, \quad t = 0 \\ &B.C: \ C = C_0, \ x = 0 \ , x = l, \ t > 0 \end{aligned} \quad (26)$$

By using of separation of variable method, we have [10]:

$$C = C_0 - \frac{4C_0}{\pi}\sum_{n=0}^{\infty}\frac{1}{2n+1}\exp\{-D(2n+1)^2\pi^2 t / l^2\}\sin\frac{(2n+1)\pi x}{l} \quad (27)$$

4 Results

In this part, first it's assumed a special situation that diffusion coefficient is constant and EFG an FEM and FDM and analytical solution in an example are compared together. Then in the second part a practical situation, which D is a function of time (m=0.2), is investigated by presenting another example.
It should be noted that due to symmetry of the practical problems, only half of the problem is solved. So in these problems only one node of the structure has Dirichlet boundary and the other node has Neumann boundary with $\frac{dC}{dt} = 0$.

4.1 Special situations

In this part, it is assumed that in the equation (2), m=0 and also annual temperature history is constant as is shown in Figure 1-b. The chloride ingress in a 1D problem is investigated.

4.1.1 Example 1:

Assuming a slab which is 1m thick and is located in the following conditions:

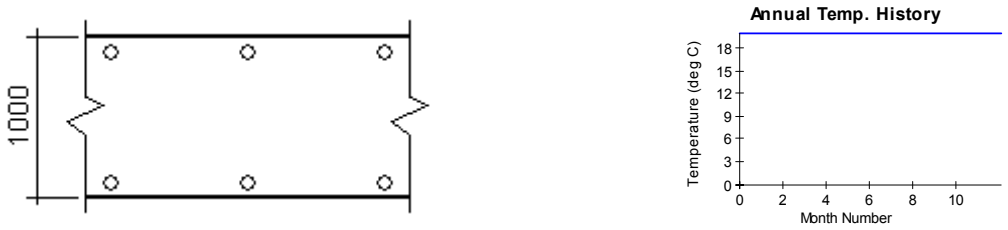

a) b)

Figure 1: a) Cross section of the slab in example 1, b) Annual temperature history

Cover = 50 mm, D = 10^{-12} m^2/s, m=0 and Ct = 0.1% (chloride by mass of concrete). Although thickness of the slab is 1000 ^{mm}, because of analyzing only half of the structure: H=500 ^{mm}.
In EFG calculations, first the scaling parameter of the support domain (d_{max}) and the weigh function's dilation parameters (K_{ch}) are optimized by using displacement error (L_2) and energy error (H_1) which are defined as the following [10]:

$$L_2 = [\int_{\Omega} (U - U^h)^T (U - U^h) d\Omega]^{1/2} \quad (28)$$

$$H_1 = [\int_{\Omega} (U_{,i} - U_{,i}^h)^T (U_{,i} - U_{,i}^h) d\Omega]^{1/2} \quad (29)$$

4.1.1.1 Results at time=20 year

The half of the slab is divided into 20 equal element or 21 nodes in FEM and the same nodes are considered for FDM and EFG method. The displacement error (L_2) and energy error (H_1) in EFG method at time=20 year with various d_{max} and K_{ch} are shown in Figures (2-5):

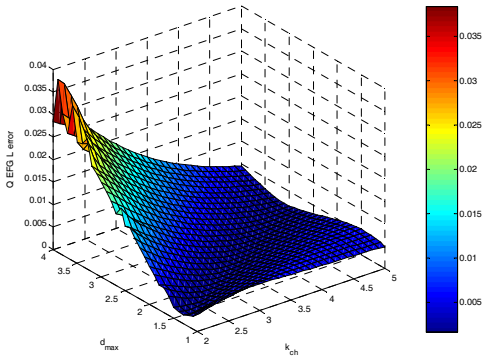

Figure 2:Q EFG L error estimation using Exponential Weight Function

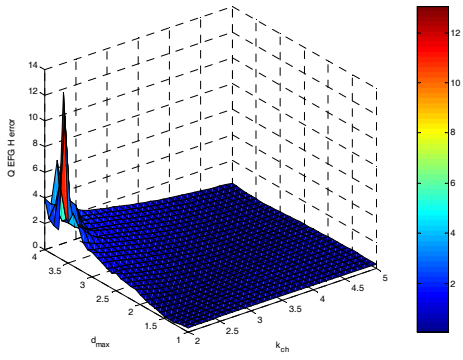

Figure 3: Q EFG H error estimation using Exponential Weight Function

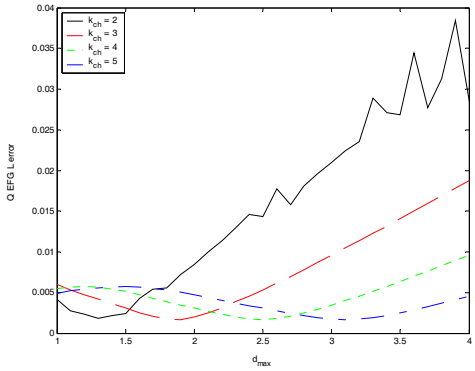

Figure 4: Q EFG L error estimation using Exponential Weight Function

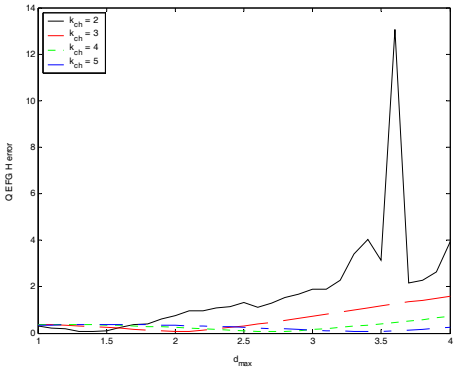

Figure 5: Q EFG H error estimation using Exponential Weight Function

It is shown that the optimum d_{max} and K_{ch} equal to 2.5 and 4, respectively. Then the Chloride-depth and its Chloride's derivative-depth and also Chloride-time are illustrated in Figures (6-8):

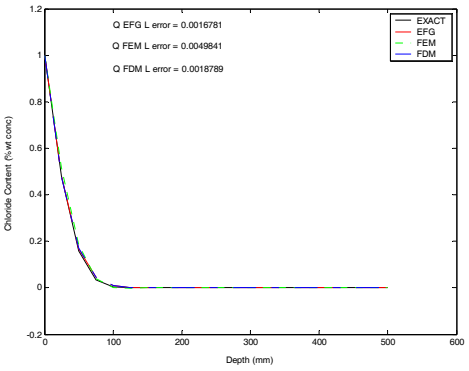

Figure 6: Concentration-Depth at Time=20years

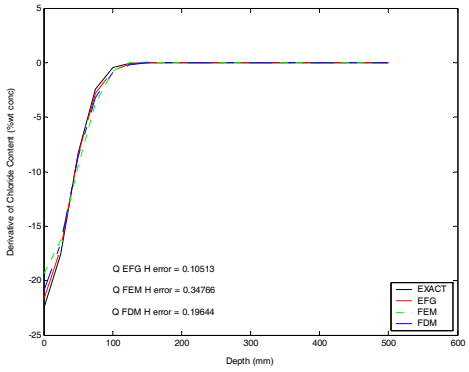

Figure 7: Derivative of Concentration-Depth at Time=20years

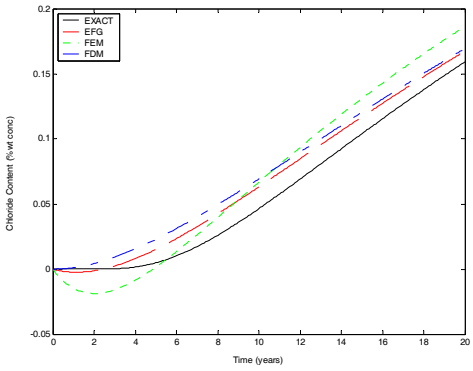

Figure 8: Concentration-Time at Cover Depth=50 mm

By dividing half of the slab into 100 equal elements, the Chloride-depth and its Chloride's derivative-depth and also Chloride-time are shown in Figurers (9-11):

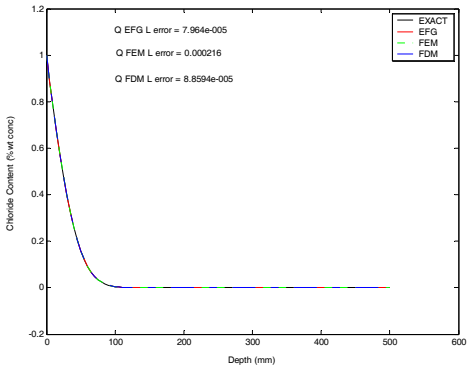

Figure 9: Concentration-Depth for Time=20years

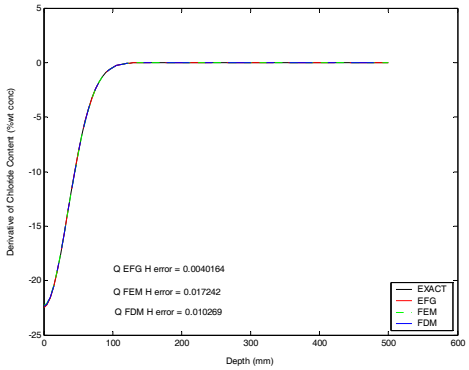

Figure 10: Derivative of Concentration-Depth for Time=20years

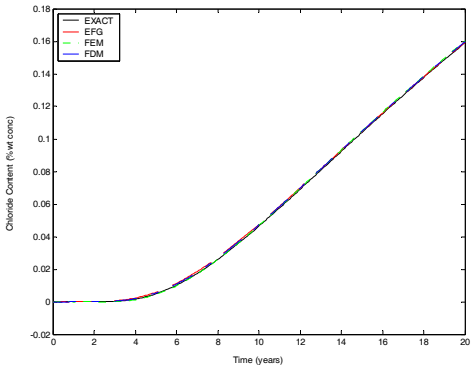

Figure 11: Concentration-Time at Cover Depth=50 mm

The displacement and energy error of FDM, FEM and EFG method are compared in table 1.

	Num. Elem.	FDM	FEM	EFG	Exact
L_2 error (%)	20	0.18789	0.49841	0.16781	-------
	100	0.0088594	0.0216	0.007964	-------
H_1 error (%)	20	19.644	34.766	10.513	-------
	100	1.0269	1.7242	0.40164	-------

Table 1: Energy and displacement errors in example 1 at time=20 year

4.1.1.2 Results at the initiation time to corrosion

If we consider the results at the initiation time to corrosion of steel bars, by dividing half of the slab into 20 equal element or 21 nodes in FEM and considering the same nodes for FDM and EFG, the results are shown in Figures (12-14).

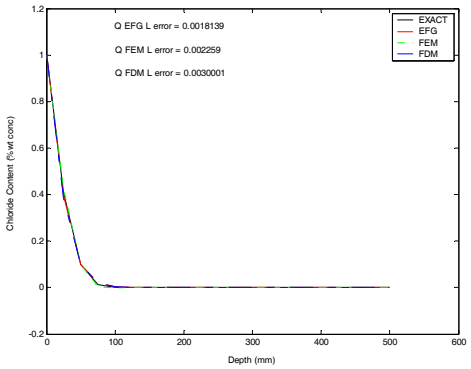

Figure 12: Concentration-Depth at the initiation time

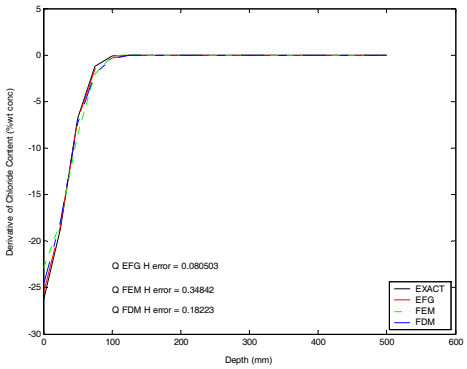

Figure 13: Derivative of Concentration-Depth

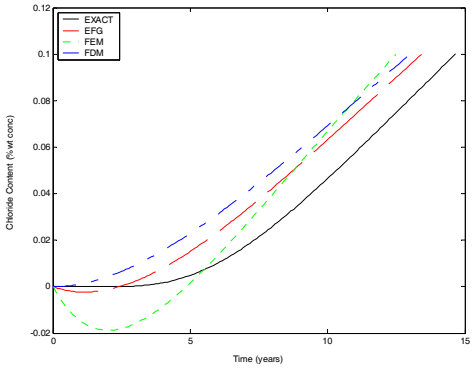

Figure 14: Concentration-Time at Cover Depth=50 mm

And by dividing into 100 elements, we have:

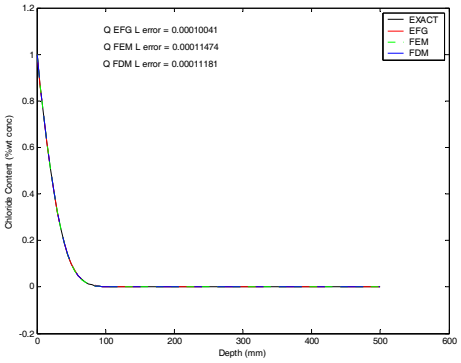

Figure 15: Concentration-Depth at the initiation time

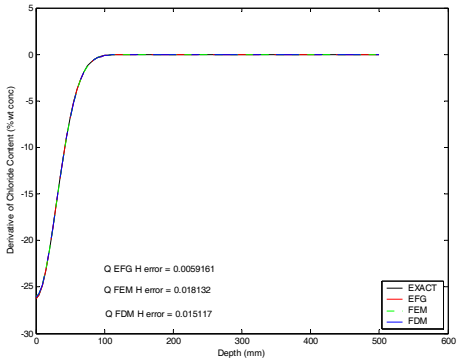

Figure 16: Derivative of Concentration-Depth

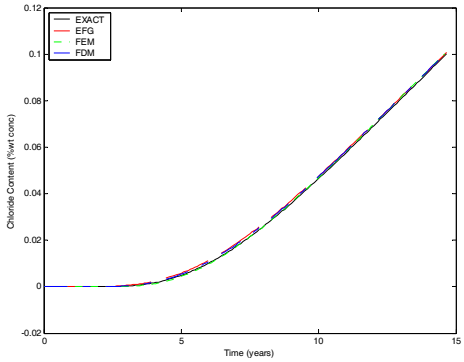

Figure 17: Concentration-Time at Cover Depth=50 mm

The ignition period to start corrosion obtained with different methods is shown in table 2.

	Num. Elem.	FDM	FEM	EFG	Exact
Initiation period (year)	20	13	12.5	13.4	14.7
	100	14.7	14.6	14.7	14.7

Table 2: The ignition period in example 1

4.2 Parctical situations

In this part we assume that diffusion coefficient is a function of time as is explained in the equation (2). So the analytical solution is not available. As we know that by increasing the elements the results converge to the exact result, we have used more elements to find the exact solution.

4.2.1 Example 2

We consider the example 1 with the Bandar-e-Abbas, Iran annual average temperature history and m=0.2 in the equation (2).

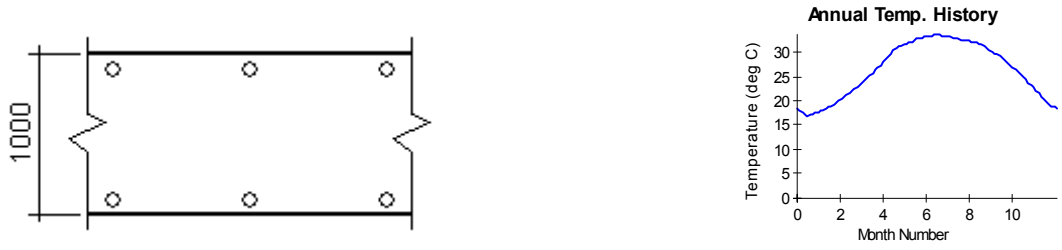

a) b)

Figure 1: a) Cross section of the slab in example 2, b) Annual temperature history

4.2.1.1 Results at time=20 year

By dividing half of the slab into 20 equal element or 21 nodes in FEM and considering the same nodes for FEM and EFG, Results at the time=10 years are shown in Figures (19-20).

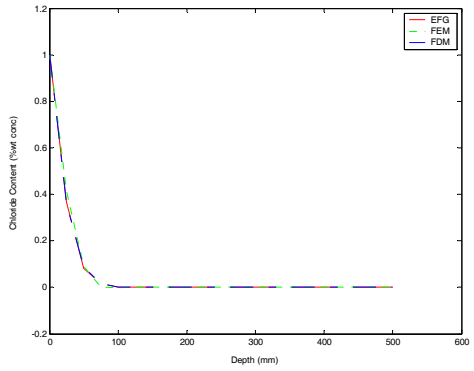

Figure 19: Concentration-Depth at Time=20years

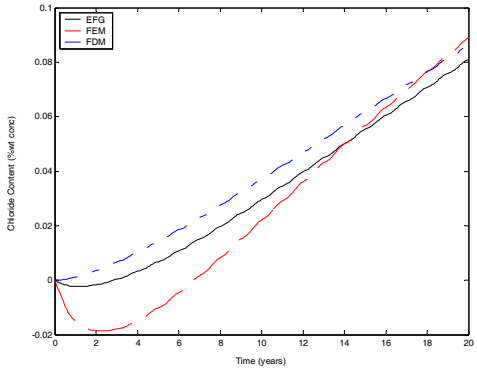

Figure 20: Concentration-Time at Cover Depth=50mm

And by dividing half of the slab into 100 equal element or 101 nodes in FEM solution and considering the same nodes for EFG solution, the results are shown in Figures (21-22).

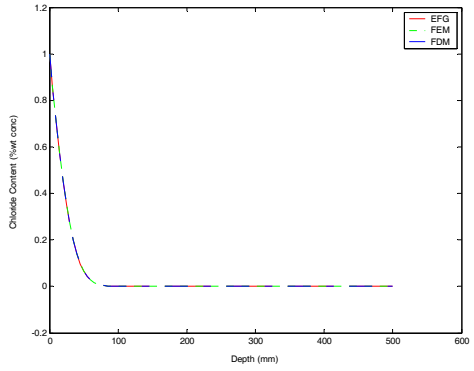

Figure 21: Concentration-Depth for Time=10years

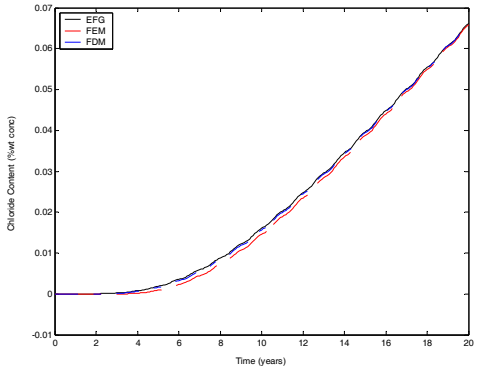

Figure 22: Concentration-Time at Cover Depth=50mm

4.2.1.2 Results at the initiation time to corrosion

By dividing half of the slab into 20 equal element or 21 nodes in FEM solution and considering the same nodes for EFG solution, Results at the initiation time to corrosion of steel bars are as shown in Figures (23-24).

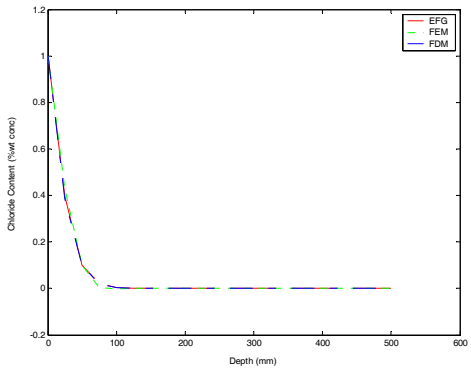

Figure 23: Concentration-Depth at the initiation time

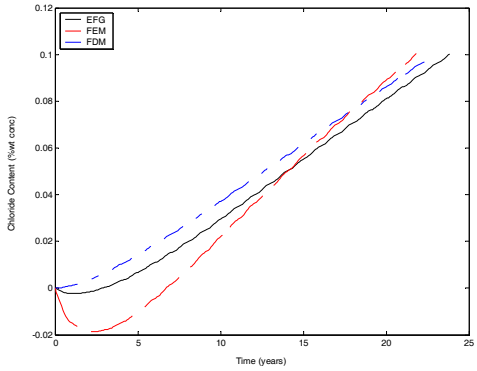

Figure 24: Concentration-Time at Cover Depth=50mm

By dividing half of the slab into 100 equal elements or 101 nodes in FEM solution and considering the same nodes for EFG solution, the results at the initiation time to corrosion of steel bars are as shown in Figures (25-26).

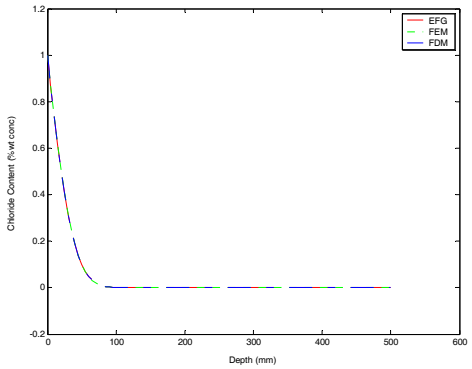

Figure 25: Concentration-Depth at the initiation time

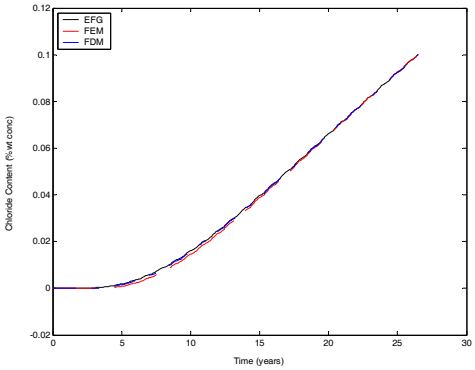

Figure 26: Concentration-Time at Cover Depth=50mm

As the previous example, the ignition period obtained with different methods are compared in table 3.

	Num. Elem.	FDM	FEM	EFG
Initiation period (year)	20	22.9	21.8	23.8
	100	26.5	26.5	26.5

Table 3: The ignition period in example 2

5 Conclusions

In this paper FDM, FEM and EFGM have been applied to solve the Fick's second low of diffusion for 1D problems. In the first step, the scaling parameter of support domain (d_{max}) and the weigh function's dilation parameters ($K_{ch)}$ to minimize the displacement error (L_2) and energy error (H_1) are optimized. Then by using these parameters in EFG method, the results are compared with the FDM and FEM and available analytical situation. It was shown that EFG method predicts the service life better than other methods and exhibits the minimum displacement error and energy error in the special situation that analytical solution is available and these errors could be found. FDM performs and its displacement error does not differ considerably with EFG method. So FDM could compete with EFG method to some extent. FEM could be used whenever the structure is divided to sufficient elements and its convergence must be always controlled.
This study for the partial differential equation of the Chloride diffusion which is a parabolic, initial boundary value problem may also used for many other physical phenomena like soil consolidation, heat transfer and others.

Acknowledgment

The financial support of the University of Tehran is acknowledged. The authors are also grateful to the material laboratory, university of Tehran. The authors sincerely thank Dr. Rahimian, and Dr. Shekarchizadeh, from University of Tehran for their technical comments.

References

[1] Oh, Byung Hwan, Jang, Bong Suk, “Chloride Diffusion Analysis of Concrete Structures Considering the Effects of Reinforcements”, ACI Material Journal, V. 100, No. 2 (2003-03)

[2] Per Goltermann, “Chloride Ingress in Concrete Structures; Extrapolation of Observations”, ACI Materials Journal: V.100, No.2 (2003-03)

[3] Thomas M.D.A. and Bentz E.C., “Manual of Life 365, Computer Program for Predicting the Service Life and Life-Cycle Costs of Reinforced Concrete Exposed to Chlorides”

[4] P. M. Gresho, R. L. Sani, “Incompressible Flow and the Finite Element Method”, Volume 1, Advection-Diffusion and Isothermal Laminar Flow, John Wiley & Sons, 2000

[5] VIANA, SA, MESQUITA, RC, “Moving Least Square Reproducing Kernel Method For Electromagnetic Field Computation”, IEEE Transactions on Magnetic, vol. 35, No. 3, May 1999

[6] Liew KM. Huang YQ. Reddy JN, “Moving least squares differential quadrature method and its application to the analysis of shear deformable plates”, International Journal for Numerical Methods in Engineering, 2003; 56: 2331-2351

[7] E. Onate, S. Idelsohn, OC Zienkiewicz, RL Taylor, “A finite point method in computational mechanics, application to convective transport and fluid flow”, International Journal for Numerical Methods in Engineering, 1996; 39:3839-3866

[8] Smolinski P, Palmer T., “Procedures for the Multi-Time Step Integration of Element-Free Galerkin Methods”, Computers and Structures 77 (2000), 171-183

[9] Crank, J., “The Mathematics of Diffusion”, Second Edition, Oxford Science Publications, Oxford, 1995

[10] Cheng-Kong C. Wu, Michael E. Plesha, “Essential boundary condition enforcement in meshless methods: boundary flux collocation method”, International Journal for Numerical Methods in Engineering, 2002; 53:499-514